NANO LETTERS

Letter

pubs.acs.org/NanoLett

Direct Imaging of a Two-Dimensional Silica Glass on Graphene

Pinshane Y. Huang,[†,■] Simon Kurasch,[‡,■] Anchal Srivastava,[§,○] Viera Skakalova,[§,∥] Jani Kotakoski,[∥,⊥] Arkady V. Krasheninnikov,[⊥,¶] Robert Hovden,[†] Qingyun Mao,[†] Jannik C. Meyer,[‡,∥] Jurgen Smet,[§] David A. Muller,*[,†,□] and Ute Kaiser*[,‡]

[†]School of Applied and Engineering Physics, Cornell University, Ithaca, New York 14853, United States

[‡]Electron Microscopy Group of Materials Science, University of Ulm, Ulm, Germany 89081

[§]Max Planck Institute for Solid State Research, Stuttgart, Germany 70569

[∥]Department of Physics, University of Vienna, Vienna, Austria 1090

[⊥]Department of Physics, University of Helsinki, Helsinki, Finland 00014

[¶]Department of Applied Physics, Aalto University, Aalto, Finland 00076

[□]Kavli Institute at Cornell for Nanoscale Science, Cornell University, Ithaca, New York 14853, United States

Supporting Information

ABSTRACT: Large-area graphene substrates provide a promising lab bench for synthesizing, manipulating, and characterizing low-dimensional materials, opening the door to high-resolution analyses of novel structures, such as two-dimensional (2D) glasses, that cannot be exfoliated and may not occur naturally. Here, we report the accidental discovery of a 2D silica glass supported on graphene. The 2D nature of this material enables the first atomic resolution transmission electron microscopy of a glass, producing images that strikingly resemble Zachariasen's original 1932 cartoon models of 2D continuous random network glasses. Atomic-resolution electron spectroscopy identifies the glass as SiO_2 formed from a bilayer of $(SiO_4)^{2-}$ tetrahedra and without detectable covalent bonding to the graphene. From these images, we directly obtain ring statistics and pair distribution functions that span short-, medium-, and long-range order. Ab initio calculations indicate that van der Waals interactions with graphene energetically stabilizes the 2D structure with respect to bulk SiO_2. These results demonstrate a new class of 2D glasses that can be applied in layered graphene devices and studied at the atomic scale.

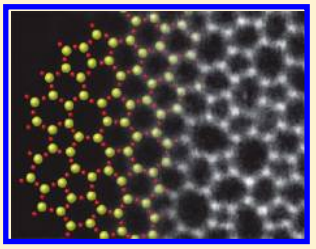

KEYWORDS: *two-dimensional glass, 2D silica, SiO_2, transmission electron microscopy, graphene imaging substrates, Zachariasen's model*

In stark contrast with two-dimensional (2D) crystals such as graphene and monolayer hexagonal boron nitride,[1] 2D glasses remain almost completely unexplored. Reducing the dimensionality of amorphous materials would enable their direct, atomic resolution structural and chemical characterization, a long-standing challenge in amorphous materials.[2−5] These materials, particularly if they can be isolated from substrates and freely manipulated, may have enormous applicability.

Figure 1a,b shows Zachariasen's original 1932 model of a continuous random network.[6] In this model, amorphous structures differ from crystalline ones simply by allowing variable bond angles, which introduce structural disorder while maintaining chemical order. In 2D, this creates amorphous structures that contain continuous networks of rings of different sizes (Figure 1b). Determining the structure of amorphous materials and comparing them to theoretical models such as Zachariasen's has remained challenging. In principle, transmission electron microscopy (TEM) and scanning TEM (STEM) possess sufficiently high resolution to resolve atomic spacings in disordered systems, particularly after recent developments in aberration-correction.[7,8] These techniques, however, typically produce images which are 2D projections of 3D structures. In these 2D projections, disorder in materials renders direct atomic-scale imaging almost impossible.[9,10]

We sidestep the projection problem by imaging a 2D glass. Crystalline two-dimensional oxides, formed from mono- or bilayers of silica tetrahedra, have recently been grown on metal substrates.[11−13] These materials are natural starting points for amorphous 2D glasses because silica is a ready glass former and contains directional bonds, a necessity for forming a disordered continuous 2D network. Here, we show that preparation of the amorphous phase of 2D silica, coupled with a graphene support,[14−16] allows atom-by-atom (S)TEM imaging and spectroscopy of a glass. During the final preparation of this manuscript, another group, using scanning tunneling microscopy, has observed an amorphous phase of 2D silica grown on bulk Ru(0001).[17] Our results demonstrate that the silica can also be grown with graphene on copper foils and isolated from the metal surface; we also detail rigorous analyses of the

Received: December 14, 2011
Revised: January 19, 2012
Published: January 23, 2012

   dx.doi.org/10.1021/nl204423x | *Nano Lett.* 2012, 12, 1081−1086

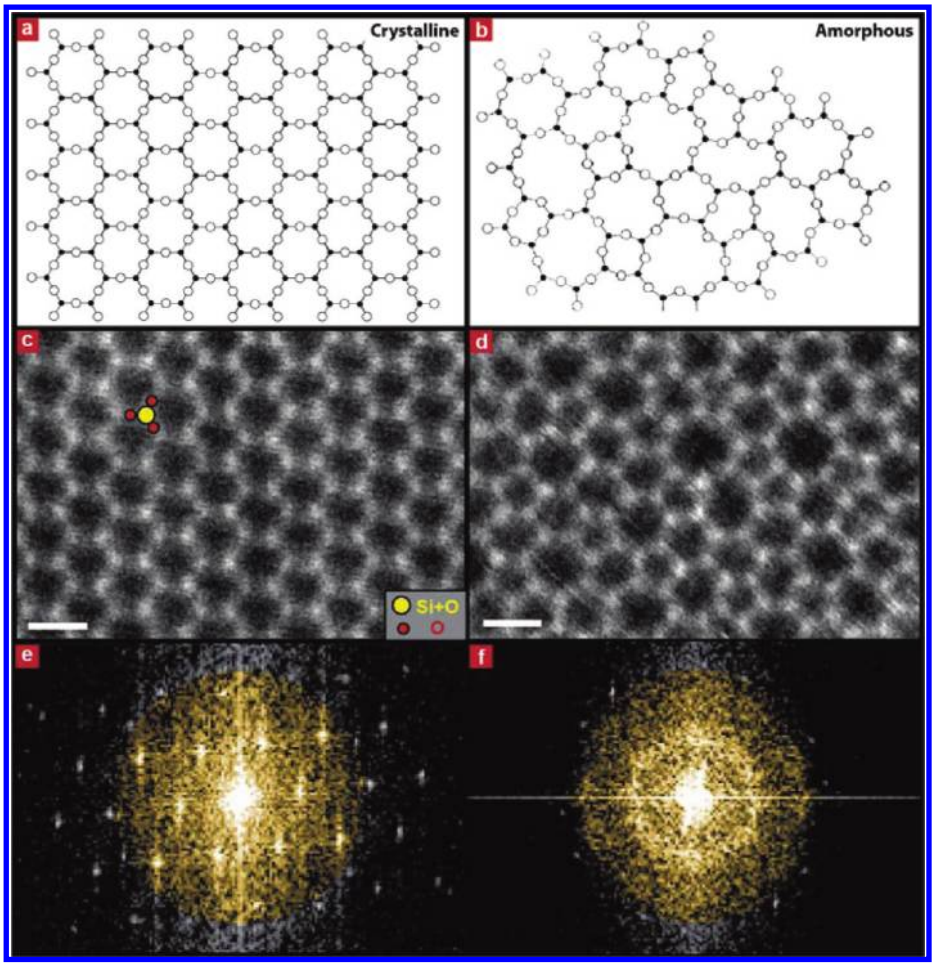

Figure 1. Atomic-resolution images of a 2D glass. (a,b) Zachariasen's models for a 2D crystal and a 2D amorphous glass, modified from ref 6. (c,d) Experimental ADF-STEM images of 2D crystalline and amorphous silica supported by graphene. The strong qualitative match between these images and Zachariasen's model suggests that these images are of a 2D glass that roughly obeys the continuous random network model. Scale bars 5 Å. (e,f) Fast Fourier transforms (FFTs) of STEM images from amorphous and crystalline regions. Spots inside the gold-colored region are from silica; spots immediately outside this region are graphene spots. Other spots can be either graphene or silica. In the silica-only (gold) regions, the amorphous silica exhibits no clear reflections, a contrast with the crystalline FFT. The silica crystalline lattice constant is 5.3 Å, roughly 2.14 times that of graphene.

structure, bonding, and thickness of the material, and the nature of the graphene–silica interface.

Figure 1c–f shows atomic-resolution annular dark-field scanning TEM (ADF-STEM) images (c,d) and corresponding diffractograms (e,f) of crystalline and amorphous regions of a 2D silica glass supported by graphene. The weakly scattering graphene substrate is not apparent in these images without filtering. As we demonstrate later, the bright spots in ADF images represent stacks of silicon and oxygen atoms, while individual oxygen atoms appear as an increase in intensity between the bright spots (see Supporting Information). The strong qualitative match between these images and Zachariasen's model suggests that these images are of a 2D glass that roughly obeys the continuous random network model. This silica was synthesized by accident during the chemical vapor deposition growth of graphene on copper foil, most likely the result of a contaminant in the graphene growth furnace (see Supporting Information). Experimentally, we have found the silica films to remain stable on graphene for over a year's exposure to air and heating to at least 400 °C in vacuum.

The diffractograms in Figure 1e,f and TEM nanodiffraction of the glass show that the crystalline lattice constant is 5.3 Å, roughly 2.14 times that of graphene (see Supporting Information). This large 7% lattice mismatch along with the presence of amorphous regions suggests that the silica is not covalently bonded to the graphene on large scales. We see no evidence for local regions that are coherently strained to be lattice-matched with the graphene. Figure 2 shows large-area TEM and STEM images of the silica. Different regions of the material range from predominantly polycrystalline (Figure 2a) to predominantly amorphous (Figure 2c) in which large areas appear to be continuous random networks. Most of the material resembles the region shown in Figure 2b, which contains mostly amorphous material with some crystalline inclusions. We attribute the mixing of crystalline and amorphous phases to growth kinetics. Additional non-silicon atoms are sometimes present in or near the center of rings, introducing small amounts of chemical disorder.

We used STEM electron energy-loss spectroscopy (EELS), which measures the local unoccupied partial density of states,[18,19] to map the composition and bonding of the glass. Figure 3a–c contains atomic-resolution maps showing the distributions of silicon, carbon, and oxygen in the region shown in Figure 3d. Figure 3 e–g shows the corresponding EEL

dx.doi.org/10.1021/nl204423x | *Nano Lett.* 2012, 12, 1081–1086

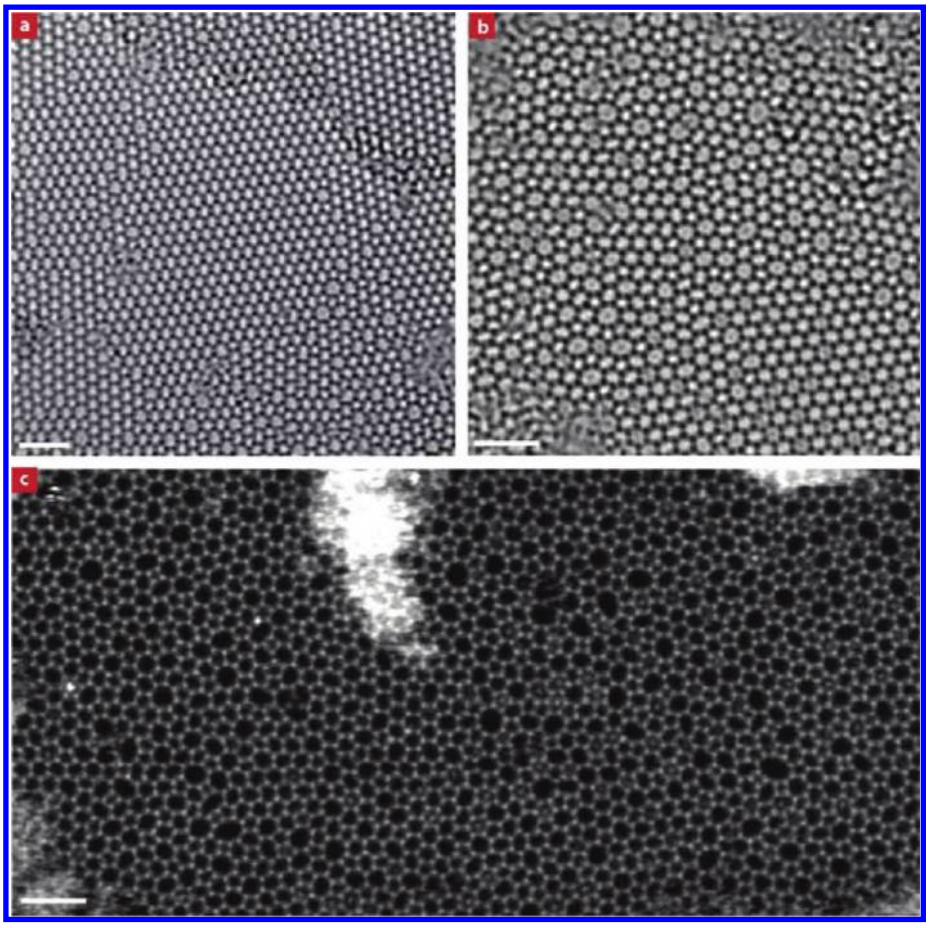

Figure 2. Large-area TEM and STEM images showing different phases of 2D silica ranging from predominantly crystalline to amorphous. (a) A smoothed TEM image of a predominantly crystalline region. Crystals are joined by grain boundaries similar to those in polycrystalline graphene.[16] (b) A TEM image of a typical region of glass, which contains both amorphous regions and crystalline inclusions such as that seen in the bottom right, which range in size from just a few unit cells up to tens of nanometers across. (c) A smoothed ADF-STEM image of an extended amorphous region formed primarily from a continuous random network of rings. Scale bars 2 nm.

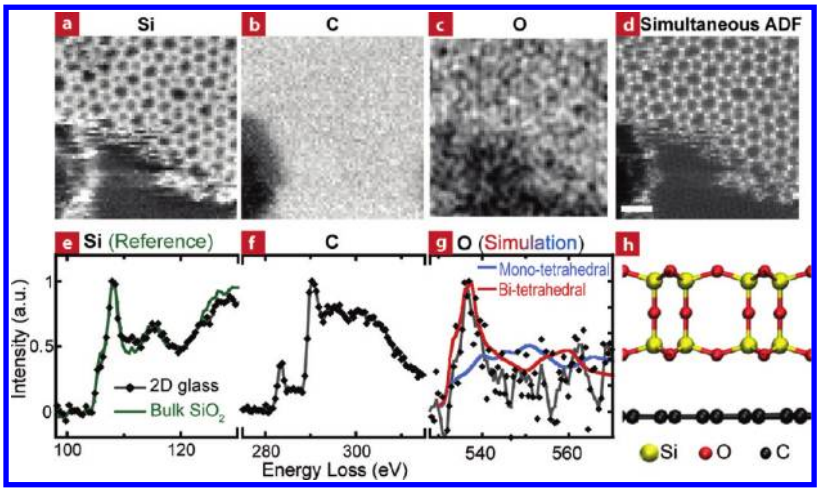

Figure 3. Atomic resolution EELS identifies the 2D glass as SiO_2, a bi-tetrahedral layer of silica. (a–c) EELS concentrations maps of Si, C, and O of a region of bilayer graphene partly covered by 2D glass (top half). The O map has been smoothed to improve contrast. (d) Corresponding ADF image. In the bottom portion of the image, the glass is damaged and largely removed with a few Si atoms clinging to the edge of the graphene sheets (bottom left). Unlike the SiO_2-like bonding in undamaged glass, these Si atoms have SiC-like fine structure, suggesting they have bonded to the graphene edge. Scale bar 2 nm. (e–g) Raw (black diamonds) and smoothed (black lines) experimental EEL spectra of the 2D glass plotted with reference data (green lines) for bulk a-SiO_2 and FEFF simulations (blue, red). (h) Side view cartoon of the structure suggested by EELS measurements.

dx.doi.org/10.1021/nl204423x | *Nano Lett.* 2012, 12, 1081–1086

spectra from the glass. The glass seen in the top portion of the ADF image corresponds with EELS maps of silicon and oxygen, suggesting that the glass is silicon oxide.

We analyzed the images and spectra in Figure 3 to construct a 3D model of the atomic structure and thickness of the silica. First, the Si-$L_{2,3}$ edges in the glass are similar to bulk SiO_2 reference EELS edges, a strong indication that the Si atoms are tetrahedrally bonded $(SiO_4)^{2-}$ units. In contrast, silicon atoms from damaged areas (Figure 3a, bottom) have a SiC-like fine structure that indicates that they have bonded to the graphene edge (Supporting Information). Additionally, the intensity and fine-structure of the C−K edge (Figure 3f) are consistent with bilayer graphene[20] and do not show any indications of covalent C−O bonding. Finally, we observe a peak at 536 eV in the O−K edge (Figure 3g). To understand the origin of this peak, we performed ab initio simulations using FEFF9[21] of two crystalline silica structural models of different thicknesses, which we term mono- and bi-tetrahedral (Supporting Information). These simulated O−K edges are plotted along with the experimental spectrum in Figure 3g. While the mono-tetrahedral structure lacks the peak observed in experiment, a good agreement is found for the bi-tetrahedral structure, shown in Figure 3h. This difference occurs because the O−K edge peaks damp out when O atoms have fewer than 6 O nearest-neighbors,[22,23] a condition met by a bilayer but not a monolayer of silica tetrahedra. Additional quantitative measurements of the amplitudes of ADF and EELS signals on the film also are within experimental error of the bilayer structure and exclude the mono-tetrahedral structure and structures which are ≥3 tetrahedra thick. (Supporting Information).

Figure 4 shows top and perspective cartoons of the bi-tetrahedral silica structure on graphene suggested by our data.

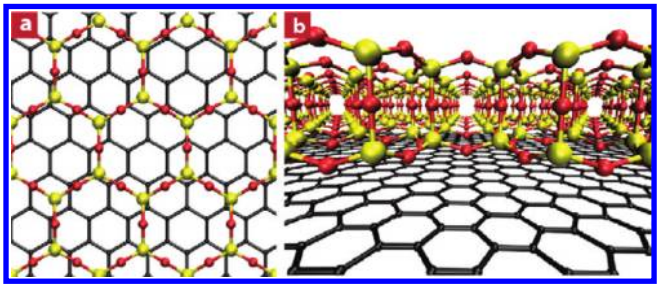

Figure 4. A structural model of 2D crystalline silica on graphene. (a) Top and (b) perspective side views of the bi-tetrahedral structure that matched experimental results.

The structural building blocks are similar to those recently reported in 2D silica on bulk Ru(0001), also composed of a bilayer of silica tetrahedra.[13,17] This structure places every atom in a local environment similar to bulk SiO_2 in which all bonds are satisfied. Unlike its crystalline analogue, the amorphous 2D silica has a unique structure where tetrahedra are disordered in two dimensions but ordered in the third dimension, where the upper and lower tetrahedra are locked in registry. This structure is therefore a 2D glass in the sense that it is single unit cell thick, analogous to 2D atomic crystals[1] such as MoS_2 or $NbSe_2$.

We extend the atomic scale analyses above by examining the pair distribution function (PDF) and ring statistics. PDFs, which statistically describe atomic spacings, have played an historic role in distinguishing between paracrystalline and continuous random network glassy models. Ring statistics are also instrumental because they can differentiate structural models whose PDFs are indistinguishable.[24,25] Ring statistics, however, are difficult, if not impossible, to measure directly in 3D glasses. These two standard metrics of structural models in glasses provide a quantitative measure of short, medium, and long-range order in our 2D glass and allow comparison to theoretical models for 2D and 3D glasses.

Figure 5a,b shows 2D-projected partial Si−Si pair-distribution functions (PDFs) in crystalline and amorphous regions

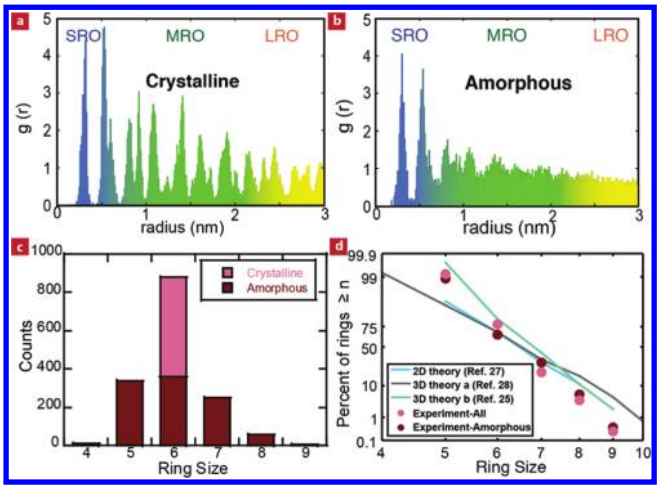

Figure 5. Structural analysis and ring statistics. (a,b) Two-dimensional projected Si−Si pair-distribution functions for crystalline and amorphous regions fully spanning the regimes of short-, medium-, and long-range order (SRO, MRO, and LRO). (c) Histogram of ring sizes and (d) ring statistics plotted on a log-normal probability scale and compared to two- and three-dimensional models.[25,27,28] None of the models fit our experimental results.

extracted from Si positions in real-space images. On short ranges, on the order of 0−5 Å, the first peak in each pair-distribution functions represents Si−Si nearest neighbor spacings. For medium ranges on the order of 5−20 Å, the pair distribution functions of the crystalline and amorphous regions begin to diverge; peaks in the amorphous Si−Si pair distributions become strongly damped. The second-peak in the amorphous PDF around 4.3 Å is almost as sharp as the first one, a notable difference from 3D silica.[26] This likely corresponds to the reduced set of possible Si−Si−Si bond angles that occur in 2D in order to provide ring closure. At long ranges >20 Å, the crystalline PDF maintains sharp peaks while the amorphous PDF is featureless.

Figure 5c plots a histogram of ring size in crystalline and amorphous regions extracted from large area images (Supporting Information). In this plot, the ring size refers to the number of vertices visible, or the projected number of tetrahedral units. In the amorphous material, we observed stable rings ranging from 3 to 10 tetrahedra in size (see Supporting Information) with an expectation value of 6.04 ± 0.024 (s.e.m.) tetrahedral units in-plane. Figure 5d compares our experimental ring statistics to a few selected theoretical models: a purely geometrical model for a 2D glass and two molecular dynamics simulations for 3D silicas using different interaction potentials.[25,27,28] None of the models fit our experimental results. Part of the deviation from the 3D models may be attributed to different dimensional geometric constraints.[29,30] Because Shackelford's 2D model takes only geometrical factors into account, we attribute its mismatch with experiment to effects not accounted for in the model, such as ring strain, formation

dx.doi.org/10.1021/nl204423x | Nano Lett. 2012, 12, 1081−1086

kinetics, and cooling rates. As direct experimental measurements of ring size distributions, these results show the distance that separates experiment and theory and should aid in improving models of connectivity in glasses.

We constructed ab initio models of a periodic bi-tetrahedral 2D silica to assess its stability, structure, and electronic properties (Supporting Information). The relaxed bi-tetrahedral structures (Figure 4) closely match our experimental results, and their calculated band structure is similar to bulk SiO_2 (Supporting Information). Our energetic calculations indicate that in vacuum, the binding energy of the bi-tetrahedral structure is 86 meV per structural unit higher than bulk silica. Adding vdW interactions to monolayer graphene energetically stabilizes the bi-tetrahedral silica over bulk SiO_2 by 107 meV per structural unit. Covalent bonding to unstrained graphene is a higher-energy state than the van der Waals bonded structures, likely because covalent bonding would result in a large 7% strain and disruption of the conjugated π-system in graphene. Our calculations therefore indicate that graphene, in addition to providing a support membrane, can stabilize new 2D materials.

Coupling ultrathin glasses with graphene support membranes frees these materials from the requirements of extreme mechanical stability, low reactivity, and isolation via exfoliation that have so far limited the range of 2D materials that could be easily identified, processed, and applied. Further, this new class of materials likely includes additional 2D glasses such as alumina or boric oxides and may be applicable in layered graphene devices. Because the silica glass can be easily removed from the copper substrate and contains no dangling bonds, it may also find application in semiconductor or layered graphene electronics as a passivated starting layer for gate insulators.

■ ASSOCIATED CONTENT

Supporting Information

Growth and sample preparation, image acquisition parameters, additional film structure information, details of elemental, bonding, and structure analysis, image simulations, and DFT structure and energetic simulations. This material is available free of charge via the Internet at http://pubs.acs.org.

■ AUTHOR INFORMATION

Corresponding Author

*E-mail: (U.K) ute.kaiser@uni-ulm.de; (D.A.M.) david.a.muller@cornell.edu.

Present Address

○Department of Physics, Banaras Hindu University, Varanasi, India 221005.

Author Contributions

■These authors contributed equally to this work.

Notes

The authors declare no competing financial interest.

■ ACKNOWLEDGMENTS

The authors acknowledge discussions with J. S. Alden, M. Antonietti, M. K. Blees, P. Cueva, M. Couillard, V. Elser, R. G. Hennig, D. M. Gatreau, S. J. Gerbode, J. W. Kevek, P. L. McEuen, J. Park, J. P. Sethna, C. S. Ruiz-Vargas, H. L. Xin, and A. M. van der Zande. Microscopy support was provided by J. Biskupek, J. L. Grazul, M. G. Thomas, E. J. Kirkland, and O. L. Krivanek.

This work was supported by the NSF through the Cornell Center for Materials Research (NSF DMR-1120296) and the National Science Foundation Graduate Research Fellowship (for P.Y.H.) under Grant DGE-0707428. U.K. and S.K. acknowledge support from the DFG (German Research Foundation) and the Ministry of Science, Research and the Arts (MWK) of Baden-Württemberg in the frame of the SALVE (Sub Angstrom Low-Voltage Electron microscopy project). J.K. and A.V.K. acknowledge the Academy of Finland for funding and CSC Finland for computational resources. A.S. acknowledges the support from Max Planck Society, Germany and Department of Science and Technology (DST), India, under the Max Planck–India fellowship. V.S. acknowledges the support from the EC Grant NMP3-SL-2011-266391 (Electro-Graph). A.S., V.S., and J.S. acknowledge support from the DFG priority program graphene.

P.Y.H. acquired and processed STEM and EELS data and conducted structure analysis, R.M.H. performed multislice images simulations, and Q.M. conducted FEFF9 simulations, all supervised by D.A.M. S.K. discovered the material, acquired and processed HRTEM and diffraction data. and participated in DFT calculations. J.C.M. contributed to HRTEM and diffraction experiments. A.S and V.S. grew the material and prepared TEM samples under supervision by J.S. J.K. and A.V.K. constructed the structural models and conceived and carried out the DFT simulations assessing the relative stability and electronic properties of the different models. U.K. supervised the HRTEM work and assembled the team. P.Y.H. and D.A.M. wrote the paper with assistance from S.K. and U.K. All contributed to the discussion of results and their implications and commented on the paper.

■ REFERENCES

(1) Novoselov, K. S.; Jiang, D.; Schedin, F.; Booth, T.; Khotkevich, V.; Morozov, S. V.; Geim, A. K. *Proc. Natl. Acad. Sci.* **2005**, *102*, 10451–10453.

(2) Wright, A.; Etherington, G.; Desa, J.; Sinclair, R. N.; Connell, G. A. N.; Mikkelsen, J. C. *J. Non-Cryst. Solids* **1982**, *49*, 63–102.

(3) Cliffe, M. J.; Dove, M. T.; Drabold, D. A.; Goodwin, A. L. *Phys. Rev. Lett.* **2010**, 104.

(4) Cockayne, D. J. H. *Mater. Res.* **2007**, *37*, 159–187.

(5) Miracle, D. B. *Nat. Mater.* **2004**, *3*, 697–702.

(6) Zachariasen, W. H. *J. Am. Chem. Soc.* **1932**, *54*, 3841–3851.

(7) Haider, M.; Uhlemann, S.; Schwan, E.; Rose, H.; Kabius, B.; Urban, K. *Nature* **1998**, *392*, 768–769.

(8) Krivanek, O. L.; Dellby, N.; Lupini, A. R. *Ultramicroscopy* **1999**, *78*, 1–11.

(9) Van Dyck, D. *Ultramicroscopy* **2003**, *98*, 27–42.

(10) Howie, A. *Philos. Mag.* **2010**, *90*, 4647–4660.

(11) Schroeder, T.; Adelt, M.; Richter, B.; Naschitzki, M.; Baumer, M.; Freund, H. J. *Surf. Rev. Lett.* **2000**, *7*, 7.

(12) Weissenrieder, J.; Kaya, S.; Lu, J. L.; Gao, H. J.; Shaikhutdinov, S.; Freund, H. J.; Sierka, M.; Todorova, T.; Sauer, J. *Phys. Rev. Lett.* **2005**, 95.

(13) Löffler, D.; Uhlrich, J.; Baron, M.; Yang, B.; Yu, X. *Phys. Rev. Lett.* **2010**, *105*, 146194.

(14) Meyer, J. C.; Girit, C. O.; Crommie, M.; Zettl, A. *Nature* **2008**, *454*, 319–322.

(15) McBride, J. R.; Lupini, A. R.; Schreuder, M. A.; Smith, N. J.; Pennycook, S. J.; Rosenthal, S. J. *ACS Appl. Mater. Interfaces* **2009**, *1*, 2886–2892.

(16) Huang, P. Y.; Ruiz-Vargas, C. S.; van der Zande, A. M.; Whitney, W. S.; Levendorf, M. P.; Kevek, J. W.; Garg, S.; Alden, J. S.; Hustedt, C. J.; Zhu, Y.; Park, J.; Mceuen, P. L.; Muller, D. A. *Nature* **2011**, *469*, 389–392.

(17) Lichtenstein, L.; Büchner, C.; Yang, B.; Shaikhutdinov, S.; Heyde, M.; Sierka, M.; Włodarczyk, R.; Sauer, J.; Freund, H.-J. *Angew. Chem., Int. Ed.* **2012**, *51*, 404–407.

(18) Egerton, R. *Electron energy-loss spectroscopy in the electron microscope*; Plenum Press: New York, 1996.
(19) Muller, D. A.; Kourkoutis, L. F.; Murfitt, M.; Song, J. H.; Hwang, H. Y.; Silcox, J.; Dellby, N.; Krivanek, O. L. *Science* **2008**, *319*, 1073−1076.
(20) Suenaga, K.; Koshino, M. *Nature* **2011**, *468*, 1088−1090.
(21) Rehr, J. J. *Rev. Mod. Phys.* **2000**, *72*, 621−654.
(22) Neaton, J.; Muller, D. A.; Ashcroft, N. W. *Phys. Rev. Lett.* **2000**, *85*, 1289−1301.
(23) Muller, D. A.; Sorsch, T.; Moccio, S.; Baumann, F.; Evans-Lutterodt, K.; Timp, G. *Nature* **1999**, *399*, 758−761.
(24) Bell, R. J.; Dean, P. *Philos. Mag.* **1972**, *25*, 1381−1398.
(25) Rino, J. P.; Ebbsjö, I.; Kalia, R. K.; Nakano, A.; Vashishta, P. *Phys. Rev. B* **1993**, *47*, 3053−3062.
(26) Tucker, M. G.; Keen, D. A.; Dove, M. T.; Trachenko, K. *J. Phys.:Condens. Matter* **2005**, *17*, S67−S75.
(27) Shackelford, J. F.; Brown, B. D. *J. Non-Cryst. Solids* **1981**, *44*, 379−382.
(28) Trachenko, K.; Dove, M. *Phys. Rev. B* **2003**, 67.
(29) Marians, C. S.; Hobbs, L. W. *J. Non-Cryst. Solids* **1990**, *119*, 269−282.
(30) Hobbs, L. W. *J. Non-Cryst. Solids* **1995**, *124*, 79−91.